Study of ZnO:V thin films prepared by dc reactive magnetron sputtering at different pressures

Liwei Wang [1,2,3]* Lijian Meng [1,2] Vasco Teixeira [2] F. Placido [4] Jinzhao Huang[3] Zheng Xu [3]

1). Departamento de Física, Instituto Superior de Engenharia do Porto, Rua Dr. António Bernardino de Almeida 431, 4200-072 Porto, Portugal.

2). Centro de Física,Universidade do Minho, Campus de Azurem, 4800-058 Guimarães, Portugal

3). Key Laboratory of Luminescence and Optical Information, Ministry of Education, Institute of Optoelectronics, Beijing Jiao Tong University, Beijing 100044, China

4). Thin Film Center, University of Paisley, Paisley PA1 2BE, Scotland

***Abstract*-Vanadium doped ZnO films with the doping concentration of 0.8% were deposited onto glass substrates at different sputtering pressures by direct current (DC) reactive magnetron sputtering using a zinc target doped with vanadium. The effect of the sputtering pressures ($5*10^{-3}$ -- $3*10^{-2}$ mbar) on the structural properties of the deposited films have been studied by X-ray diffraction (XRD), scanning electron microscopy (SEM) and Energy Dispersive Spectrometry (EDS). The results of XRD show that all the films have a wurtzite structure and grow mainly with the c-axis orientation. The residual stresses which have been estimated by fitting the XRD results decrease with increasing sputtering pressure. The optical properties of the films were studied by measuring the transmittance. The optical constants (refractive index and extinction coefficient) and the film thickness were obtained by fitting the transmittance. All the results are discussed in relation with the sputtering pressure and the doping of the vanadium.**

I. Introduction

ZnO is a wide band gap semiconductor with optoelectronic properties that make it an attractive candidate for a variety of device applications[1]-[4] . Diluted magnetic semiconductors (DMS) have recently attracted great attention because of their potential application for spintronics devices[5]. In DMS materials, transition or rare earth metal ions are substituted onto cation sites of the host semiconductor and are coupled with free carriers to introduce ferromagnetism [6],[7]. K. Sato et al , predicted that ZnO doped with Cr, Fe, Co, V and Ni can be ferromagnetic [8]-[11]. Recently, some experimental work show that V doped ZnO can introduce ferromagnetism (FM). However, so far, not much work has been done about this. There have been some reports of ZnO:V films prepared by magnetron sputtering [12] , pulsed laser deposition [13],[14] , ion plating [15] , etc. Among the deposition techniques, DC reactive magnetron sputtering technique has some advantages in comparison to the other methods[16]. This technique is quite simple and the required equipment is less expensive, and is considered to be the most favorable deposition method to obtain highly uniform films with high packing density and strong adhesion at a high deposition rate.

In the present work we have studied the influence of the total pressure on the structural and the optical properties of the ZnO:V thin films prepared by dc reactive magnetron sputtering. It has been found that the structural and the optical properties are strongly dependent on the processing conditions.

* Email: wangleewei@hotmail.com

II. Experiment

ZnO:V thin films were deposited on the glass substrate by DC magnetron sputtering using Znic (99.99%) metal target with some pieces of vanadium. The distance between the target and the substrate was 50 mm. The sputtering chamber was evacuated to a base pressure below $3*10^{-5}$mbar. The target were well cleaned and etched for 5 min with pure Ar atmosphere using the current of 0.3A and the substrate was covered with the shutter in the chamber before deposition. During sputter deposition, the sputtering current applied to the target was fixed at 0.3A. The substrate temperature was kept at room temperature. The sputtering gas Ar with a purity of 99.99% and the reactive gas O_2 with a purity of 99.99% were introduced to the chamber separately and controlled by the standard mass flow controllers. The deposition pressure were $3*10^{-2}$, $1.5*10^{-2}$, $9*10^{-3}$, $7*10^{-3}$ and $5*10^{-3}$ mbar at the constant oxygen partial pressure $3*10^{-3}$ mbar.

The crystal structures of the films were characterized by XRD, using a Cu Kα radiation source and the scanning range from 10° to 80°. Peak position and the peak intensity were obtained by fitting the measured peaks with two Gaussian curves in order to get the true peak position and intensity corresponding to monochromatic Cu Ka1 radiation. The surface morphology and cross-section microstructure of the films were observed by SEM and the stoichiometries of the films were determined by EDS. The transmittance spectra were measured in the range of 300–2500 nm wavelength using a Shimadzu UV-3101PC spectrophotometer.

III. Results and discussion

A Structural properties

Vanadium concentration in ZnO films deposited at

978-1-4244-1573-1/08/$25.00 © 2008 IEEE

different sputtering pressures has been detected by EDS measurement. It has been found that the doping concentration is about 0.8 mol % and is same for all samples.

Fig. 1 shows the XRD patterns of the ZnO:V thin films deposited on glass substrates at different pressure with an oxygen partial pressure of $3*10^{-3}$mbar. The XRD has been done at 2θ between 10º to 80º. As only (002) and (004)peak is observed for all samples. The XRD results indicate that all the samples are wurtzite structure. This result implies that a few of V impurities doesn't change wurtzite structure of ZnO. It can be seen also that vanadium doped ZnO films have a preferred c-axis orientation of ZnO. The c-axis orientation in ZnO:V films can be understood by the ''survival of the fastest'' model proposed by Drift [17]. According to this model, nucleations with various orientations can be formed at the initial stage of the deposition and each nucleus competes to grow but only nuclei having the fastest growth rate can survive, i.e., c-axis orientation is achieved.

In addition to the c-axis orientation, a small shift of the peak position of the (002) plane is observed with the variation of deposition pressure as shown in the inset graph of Fig.1 and the 2θ value for all the films is found to be less than the unstressed pure ZnO powder value[18] . It indicate that the value of c-axis lattice parameter for the ZnO:V films is large in comparison with unstressed bulk value of 2.6033 Å[18]. The large value of lattice constant for the ZnO:V thin films compared to the unstressed powder value shows that the unit cell is elongated along the c axis, and compressive forces act in the plane of the film. The residual stress of the films were calculated from the value of lattice parameter of film using the expression by (1) [19]

$$\sigma = \frac{2c_{13}^{2} - c_{33}(c_{11} + c_{12})}{2c_{13}} \frac{d - d_{0}}{d_{0}} \qquad (1)$$

where d is the crystallite plane spacing of the films, and d0=2.6033Å is the standard plane spacing from X-ray diffraction The values of the elastic constant from single crystalline ZnO are used, C11=208.8 GPa, C33=213.8 GPa, C12=119.7 GPa and C13=104.2 GPa. Substituting these values in the above equation gives σ=-233(d-d_0)/ d_0. The

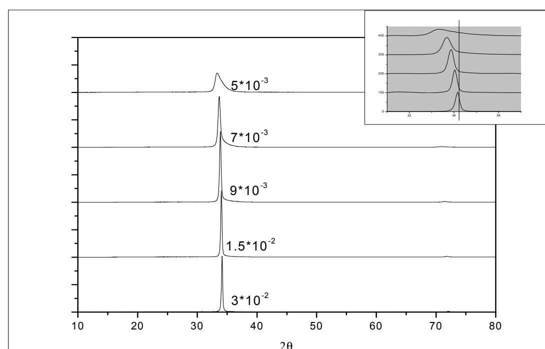

Fig. 1. X-ray diffraction pattern of films prepared at different sputtering pressures. The inset graph shows the XRD pattern with 30≤2θ≤40

TABLE I

Grain size along (002) direction, residual stress and thickness of the ZnO:V films prepared at different sputtering pressures

Sputtering pressure (mbar)	Thickness (nm)	FWHM (degree)	d(Å)	Stress (Gpa)	Grain size(nm)
$3*10^{-2}$	782	0.19	2.6260	-2.03	46
$1.5*10^{-2}$	1473	0.22	2.6352	-2.86	40
$9*10^{-3}$	1434	0.28	2.6481	-4.00	30
$7*10^{-3}$	1250	0.42	2.6626	-5.30	20
$5*10^{-3}$	1023	0.76	2.6937	-8.09	11

calculated residual stresses of the films are shown in Table 1. From Table 1 it can be seen that all the samples have a negative residual stress which indicates a compressive stress in the films. The residual stress of the films increases with the decrease of sputtering pressure. The large value of lattice parameter may be attributed to the incorporation of defects in the form of interstitial oxygen during deposition. During the deposition, the energy of the sputtered particles arriving at the substrate surface raised with decreasing the pressure. This can generate more defects, holes and substituted atoms which can expand the volume to make residual stress the greater.

The full width at half maximum (FWHM) of (002) x-ray peak was found to decrease with increasing of the sputtering pressure. The average crystallite dimension of films, D, was calculated using the (2)[20]

$$D = \frac{0.9\lambda}{B\cos\theta} \qquad (2)$$

where λ is the X-ray wavelength, θ is the Bragg diffraction angle and B is the full width at half maximum(FWHM) after correction for the instrument broadening. By fitting the measured X-ray diffraction data, the average crystallite size of the films has been calculated from diffraction peak of (002). The calculated grain sizes are shown in Table 1. Crystallites size in the direction of vertical the substrates of the films prepared at high sputtering pressure is larger than that of films prepared at low sputtering pressure. So it can be found that the films, which have large crystallites, have low residual stress. This is because the films, which have large crystallites, have less dislocation and crystallite boundaries. Compared with the crystallite of pure ZnO film[21], Vanadium doped in ZnO films will stimulate the grain growth of ZnO films and make the doped films have larger crystallite sizes, which improve the crystallinity of ZnO films. This phenomenon has been found in the experiments with Tb-doped ZnO films and Ga doped ZnO films [22],[23].

B Surface morphology

Fig.2 shows the SEM surface and cross-section morphology of the ZnO:V thin films deposited at different total pressures. It can be seen that the average of grain size along the surface and the roughness of film increase with the raising of sputtering pressure and the films have a normal columnar structure as observed from the cross-section. The grain size vertical the surface also increase with the sputtering pressure. These agree with the calculated result of XRD.

From Fig.2 it can be seen that the film prepared at high total pressure has more porous structure than the film prepare at low pressure. As the total pressure is raised, the energy of the

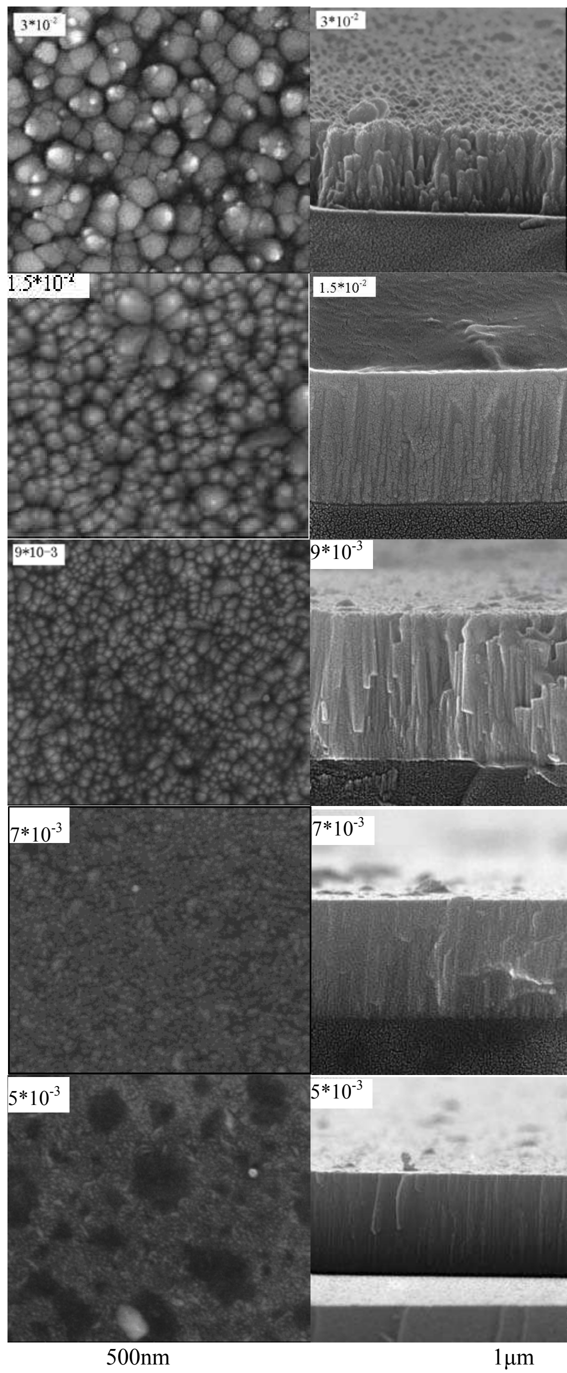

Fig. 2. SEM micrographs of films prepared at different sputtering pressures.

sputtered particles arriving at the substrate surface falls because of collisions with the gas components, leaving less energy for surface diffusion. This will result in a decrease of the surface mobility of the sputtered particles on the substrate. Usually, low surface mobility is connected with 3-D island growth, whereas high surface mobility means that the growth of the film take place in a more or less 2-D manner, completing a monolayer before the second layer begins to form. So the dense packing structure was formed for the films prepared at low sputtering pressure and the porous structure was formed for the films prepared at high sputtering pressure.

C. *Optical properties*

Fig. 3 shows optical transmittance spectra of the ZnO:V films. As can be seen from Fig.3, the transmittance increases with increase of sputtering pressure. The absorption edge of the transmittance for the film prepared at $3*10^{-2}$mbar shifts to the shorter wave length, i.e., blue shift.

The thickness, refractive index and extinction coefficient of films were obtained by fitting from the transmittance spectra using the Drude Model and OJL model[24],[25].

The calculated refractive indices of all ZnO:V thin films are shown in Fig.4(a). The decrease of refractive index indicates the decrease of the density of the films with the increase of sputtering pressure. That means the film density decrease as the pressures are increased. This leads to the decrease of the refractive index. From Fig. 2 it can be seen that samples at higher pressure is formed by disordered nano-rods, the space between these nano-rods results in a low packing density and subsequently a low refractive index. The index of refraction, n, become less when increasing the sputtering gas pressure during deposition. This can be easily understood as a thermalization effect. The sputtered particles lost their initial high energy due to collisions with gas atoms and become thermalized. This reduces the adatom mobility at surface of the growing film and leads to a porous film structure due to a shadowing effect. Consequently the index of refraction, n, is reduced. [26]

It is observed that the refractive index of the ZnO:V thin films are smaller than that of the pure ZnO film in the measured wavelength range[21],[27]. The decrease in refractive index is attributed to the deceasing of the value of

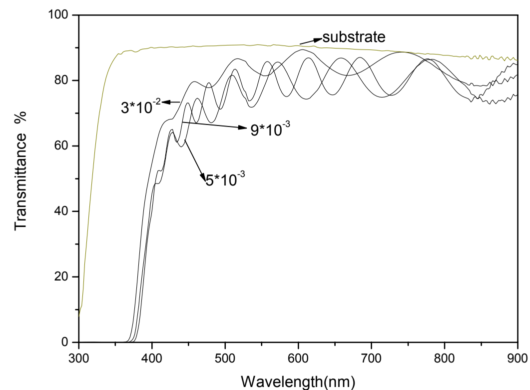

Fig. 3. Transmittance spectra of films prepared at different sputtering pressures.

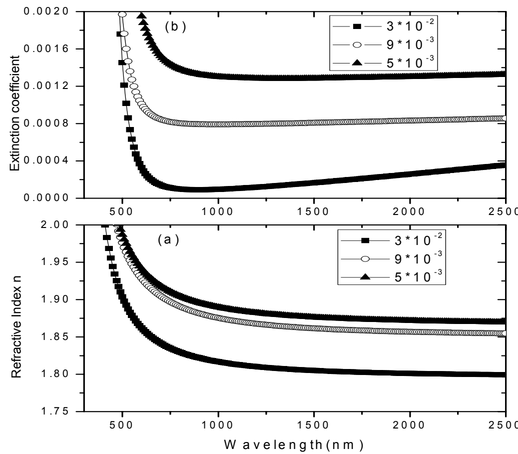

Fig. 4. a) The refractive index and
b) The extinction coefficient of the films with different sputtering pressure

grain size and an increase in the porosity of ZnO:V thin film.

Fig. 4(b) shows the extinction coefficient of films prepared at different sputtering pressures. The scattering centre concentration decreases with the increase of sputtering pressure due to the increase of the crystallite size with the increase of sputtering pressure. the light loss introduced by scattering increasing. In our films, the scattering mainly results from oxygen vacancies and grain boundaries. The films which have big grain size should have small scattering coefficient. Comparing with Table 1, it is true for our films. Hence the extinction coefficient increases with the increase of sputtering pressure.

To obtain the band gap E_g, we have used Tauc et al.'s plot [28] where the absorption coefficient α is a function of the incident energy and optical band gap Eg is given by

$$\alpha=A(h\nu-E_g)^{1/2}/h\nu \quad (3)$$

$$T=(1-R)e^{-\alpha t} \quad (4)$$

where A is a function of refractive index of the material, reduced mass and speed of light. *T* is the transmittance of the thin film, *R* the reflectance and *t* the thickness of the film obtained from the simulation. Since the reflectivity is negligible and insignificant near the absorption edge. $(\alpha h\nu)^2$ is a function of the energy of incident radiation .The energy band gap can be evaluated from the linear part of the curve with the energy axis. The optical energy band gap of the films decreased from 3.34, 3.32 to 3.31 eV with decreasing the sputtering pressure. This may be due to different effects, but the most relevant are grain size, lattice strain or defect states.

IV. Conclusion

ZnO:V thin films were deposited on glass substrate by dc reactive magnetron sputter. The structural and optical properties of the ZnO:V thin films are dependent on the sputtering pressure.

The films have highly preferred orientation with *c*-axis perpendicular to the substrate at higher sputtering pressure. The grain sizes are increasing with the sputtering pressure and the stain of all the samples have a compressive stress which increases with decreasing the sputtering pressure. The XRD patterns of the samples indicated that the crystallites of the ZnO:V thin films grown at higher sputtering pressure were good quality.

The average transmittance for all prepared samples is about 80% in the wavelength range of the visible spectrum. The refractive index and extinction coefficient–wavelength dependence was calculated from the transmission spectra. With lessening of sputtering pressure, the refractive index and extinction coefficient both decreased.

The thickness, refractive index and extinction coefficient of films were obtained. The transmittance drops and refractive index decreases and extinction coefficient rises with the decreasing of sputtering pressure. The refractive index of the ZnO:V thin films are smaller than that of the pure ZnO film in the measured wavelength range. The optical bandgap was found to increase with increasing sputtering pressure.

Acknowledgment

The authors are grateful to the NSFS(60576016), 863 program (2006AA03Z0412), BNSFC(2073030), 973 Program (2003CB314707), NSFC(10434030) and Beijing Jiao Tong University Doctor Science Creative Grants No. 48027.

References

[1] Roeksabutr, A.; Chu, P.L.;Lasers and Electro-Optics Society Annual Meeting, 1997. LEOS '97 10th Annual Meeting. Conference Proceedings., IEEE. 2(1997) 124 - 125
[2] Y.C. Kong, D.P. Yu, B. Zhang, W. Fang, S.Q. Feng, Appl. Phys. Lett. 78 (2001) 407.
[3] Won Il Park, Dong-Wook Kim, Sug Woo Jung, Gyu-Chul Yi. Int. J. of Nanotechnology. 3(2006) 372 - 395
[4] Chia Ying Lee; Seu Yi Li; Pang Lin; Tseung-Yuen Tseng; Nanotechnology, IEEE Transactions . 5 (2006) 216 - 219
[5] S. A. Wolf, D. D. Awschalom, R. A. Buhrman, J. M. Daughton, S. von Molnár, M. L. Roukes, A. Y. Chtchlkanova, and D. M. Treger, Science 294(2001) 1488.
[6] T. Dietl, H. Ohno, F. Matsukura, J. Cibert, and D. Ferrand, Science 287(2000)1019.
[7] Geun Young Ahn; Seung-Iel Park; Kim, S.J.; Bo Wha Lee; Chul Sung Kim. Magnetics, IEEE Transactions. 41 (2005) 2730 – 2732
[8] Sato K, Katayama-Yoshida H , Jpn. J. Appl. Phys Part 2-LETTERS 39 (6B) (2000) L555-L558.
[9] Sato, K, Katayama-Yoshida, H, Yamamoto, Mater Res Soc Symp 623 (2000) 65-75.
[10] Sato, K, Katayama-Yoshida, H , Pysica E 10 (1-3) (2001) 251-255.
[11] K. Sato and H. Katayama-Yoshida, Jpn. J. Appl. Phys.40, (2001). L334 .
[12] Ruan Yi-Bin, Meng Li-Jian, Liang Er-Jun. Chinese Journal of Inorganic Chemistry. 22(12) 2006 2247-2252.
[13] Y. Ishida, J.I. Hwang, M. Kobayashi, A. Fujimori, H. Saeki, H. Tabata, T. Kawai, Physica B351 (2004) 304.
[14] N.H. Hong, J. Sakai, A. Hassini, J. Appl. Phys. 97 (2005) 10D312.
[15] A.F. Vyatkin, V.I. Zinenko, Yu. A. Agaphonov, A.N. Pustovit, D.V. Roshchupkin, F. Reuss, C. Kirchner, R. Kling, A. Waag, Nucl. Instrum. Method. Phys. Res. B237 (2005) 179.
[16] Z.Z. Ye, J.F. Tang, Appl. Opt. 28 (1989) 2817.
[17] A. Van der Drift, Philips Res. Rep. 22 (1967) 267.
[18] American Standard for Testing of Materials _ASTM_ 36–1451.
[19] Y. G. Wang, S. P. Lau,a) H. W. Lee, S. F. Yu, B. K. Tay ,X. H. Zhang ,K. Y. Tse , H. H. Hng J. Appl. Phys. 94, (2003) 1597-1604.

[20] B.D.Cullity,Elements of X-ray Diffraction. 2nd ed.(Addison-wesley,Reading,MA,1978).
[21] Li-Jian Meng, M.P. dos Santos. Thin Solid Films 250 (1994) 26-32.
[22] Z.B. Fang, Y.S. Tan, H.X. Gong, C.M. Zhen, Z.W. He, Y.Y. Wang, Mater. Lett. 59 (2005) 2611.
[23] Quan-Bao Ma, Zhi-Zhen Ye, Hai-Ping He, Shao-Hua Hu, Jing-Rui Wang, Li-Ping Zhu, Yin-Zhu Zhang, Bing-Hui Zhao Journal of Crystal Growth. 304(2007), 64-68.
[24] A. Solieman and M.A. Aegerter Thin Solid Films 502(1-2), (2006), 205-211.
[25] M. Theiss, Hard and Software for Optical Spectroscopy, Dr. Bernhard-Klein-Str. 110, 52078 Aachen, Germany .
[26] P.Lobl, M.Huppertz, D.Mergel. Thin Solid Films 251(1994)72-79.
[27] J. Tauc, R. Grigorvici and A. Vancu, Phys. Status Solidi **15** (1966), 627.